*Metallurgical and Materials Engineering* *Research paper*
*Association of Metallurgical Engineers of Serbia AMES* *https://doi.org/10.30544/761*

# SANDWICH COMPOSITE OF ALUMINUM ALLOY AND MAGNESIUM ALLOY THROUGH ACCUMULATIVE ROLL BONDING TECHNIQUE

*J Aishwarya, M. Nithin Kumaar, R. Vaira Vignesh*[*]*, M. Govindaraju*

*Department of Mechanical Engineering, Amrita School of Engineering, Coimbatore, Amrita Vishwa Vidyapeetham, India*

*Received 10.11.2021*

*Accepted 17.06.2022*

## Abstract

Aluminum and magnesium alloys are lightweight materials with outstanding technical uses. Due to their combined qualities, composites built of aluminum and magnesium alloys have surpassed the utilization of these elements individually. Accumulative Roll Bonding was used to create a three-layered sandwich composite structure made of Al-alloy/Mg-alloy/Al-alloy. The composite structure's microstructure and mechanical characteristics were studied. A fine-grained AZ31 layer was formed, according to the microstructural study. At the Al-alloy/Mg-alloy contact, a diffusion layer was also seen. On the broken surface, fractography exhibited both ductile and brittle failure characteristics.

**Keywords**: lightweight; sandwich composite; accumulative roll bonding; diffusion layer; fractography.

## 1. Introduction

Since the beginning of the 20$^{th}$ century, there has been a rush in the creation of improved lightweight materials [1]. In recent years, lightweight materials have found amazing uses in several sectors. [2-4] Among these are the maritime, automotive, and aerospace sectors. With the dawn of the 21$^{st}$ century, the requirement for these lightweight materials to replace heavy applications in order to improve performance has become unavoidable. The demand for lightweight materials is continually increasing due to the automobile industry's projected emission reduction rules [5]. These materials serve a vital role in saving the economy and the environment, as well as boosting the performance and durability of the goods. Recently, aluminum and magnesium alloys have dominated the lightweight material sector [6, 7]. They have a low density and a high ratio of strength to weight.

[*] Corresponding author: R. Vaira Vignesh, *r_vairavignesh@cb.amrita.edu*

Their simplicity of processing and fabrication, as well as their many other distinctive qualities, have made them a superior alternative for numerous engineering applications. Al can reduce the total mass of the structure by up to 60%, while Mg can reduce the mass by up to 70% if the building is formed from ferrous components. Several studies demonstrate that Al alloys are an effective substitute for several steel and cast-iron components [8-10]. Numerous studies are conducted on Mg alloys to investigate their numerous industrial and non-industrial applications [11-13]. Consequently, composites comprised of both Al and Mg exhibit different properties of both materials and have a broad range of applications.

Composite structures, such as sandwich panels and honeycomb structures, feature adhesive material bonds [14]. Sandwich composites offer the structure with rigidity and flexural strength while maintaining its lightness. However, the production of such composite structures can be laborious. Using the Severe Plastic Deformation (SPD) technique is a straightforward way to construct such composite structures. Accumulative Roll Bonding (ARB) is an SPD technique that facilitates the fabrication of such stacked structures [15]. It is one of the growing procedures that refines grains and boosts the composite's yield strength [15, 16]. In recent years, extensive study has been conducted on the ARB approach for producing sandwich structures from metal alloys. The production of a lightweight construction with integrated material properties is vastly possible with these designs.

Multiple studies demonstrate that ARB improves the grain characteristics of the material. According to *Rahmatabadi et al.* [17], the microhardness of the layers increased with the number of passes. The creation of new high-angle grain boundaries aided in the composite's grain refining. *Gholami et al.* [18] investigated the effect of applied strain and volume percentage of components in multilayered Al/Mg composites manufactured by the ARB method. They observed the necking of Mg during the earliest rolling stages. Increasing the number of ARB cycles improved the material's mechanical characteristics. *Jafarian et al.* [19] have demonstrated that as the number of ARB cycle passes increases, so does the composite's strain-hardening capacity. Using the ARB method, *Rahmatabadi et al.* [20] created Al/Mg-Li composite. According to microstructural investigations, the bonding between layers enhanced when the strain rate was high. *Wang et al.* [21] discovered that the grain size of the final composite dropped dramatically as the number of ARB cycles increased. During the process, shear strain also contributes to the ultra-fine refining of the grain structure.

In the present study, an Al-alloy/Mg-alloy/Al-alloy-based sandwich composite structure was developed by ARB technique at ambient temperature. This work focuses on fabricating a single sandwich composite structure with aluminum alloy AA7075 sandwiching the magnesium alloy AZ31. The microstructural evolution and mechanical properties were examined.

## 2. Materials and Methods

### *2.1 Materials*

As raw materials for the current work, aluminum alloy (AA7075) and magnesium alloy (AZ31) plates were used. Initially, the plates had a thickness of 4 mm. Table 1 provides the chemical composition of the primary components.

***Table 1.*** *Chemical composition of the base materials.*

| Material | Composition (in weight %) |
|---|---|
| AA7075 | Al 97.76, Cr 0.06, Cu 0.19, Fe 0.25, Mg 0.8, Mn 0.12, Zn 0.11, Si 0.7 |
| AZ31 | Mg 95.8, Al 3, Zn 1, Mn 0.2 |

*2.2 Rolling*

In order to improve their ductility during the rolling operation, the alloy plates were annealed and then rolled into alloy strips before to the ARB process. The AA7075 alloy underwent two sequential annealing processes. In the first phase of the annealing procedure, the alloy plates are immersed in an inert environment (Argon) at 425°C for two hours. The second step includes soaking the alloy plates in an inert environment (Argon) at 230°C for two hours. Plates of annealed AA7075 alloy were cold-rolled to a thickness of 0.7 mm to produce an 82.5% reduction in thickness. Plates of AZ31 alloy were annealed for 15 minutes at 345°C in an inert environment (Argon). The annealed AZ31 alloy sheets were later hot rolled at 410°C to a thickness of 2 mm, resulting in a 50% reduction in thickness.

*2.3 Accumulative Roll Bonding*

The alloy strips underwent a second heat treatment (annealing) to alleviate tensions and reduce hardness introduced during the rolling process. The alloy strips were annealed according to the parameters outlined in the preceding section. The alloy strips were washed and degreased with acetone and then mechanically scratched with a wire brush to remove oxide deposits from the surface. The alloy strips of dimensions 25 mm x 50 mm x thickness (AA7075 – 0.7 mm; AZ31 – 2 mm) were layered on top of one another. The mechanical scratching between the metal strips ensured a strong surface contact. Figure 1 is a diagram of the ARB approach. Equal-sized metal strips were placed onto one another to produce a sandwich structure. A strip of AA7075 alloy was sandwiched between two strips of AZ31 alloy to form the sandwich structure. At 400°C, the sandwich structure was hot-rolled through. The sandwich structure was hot-rolled at 400°C in four passes, with at least 50 percent thickness decrease in each pass, to generate an AA7075 alloy and AZ31 alloy accumulative roll-bonded sandwich structure.

*2.4 Characterization using analytical instruments*

The elemental composition and the elemental map were determined using the Energy Dispersive X-ray Spectroscope (EDS; Make: Oxford Instruments; Model: Ultim Max).

*2.5 Microstructure*

The ARB composite was sliced along the transverse section and mounted using a cold-setting adhesive. Using an automatic disc polisher and standard metallographic sheets, the specimen was polished. The specimens were then finely polished with alumina suspension using an automatic disc polisher. The specimen was etched with Barker's reagent, the usual etchant (5mL HBF4 and 200 mL H2O). Barker's reagent was made in accordance with the ASM handbook's [22] instructions. Using an inverted metallurgical optical microscope, the transverse section of the material was examined for its microstructure (Make: Carl Zeiss; Model: Axiovert 25).

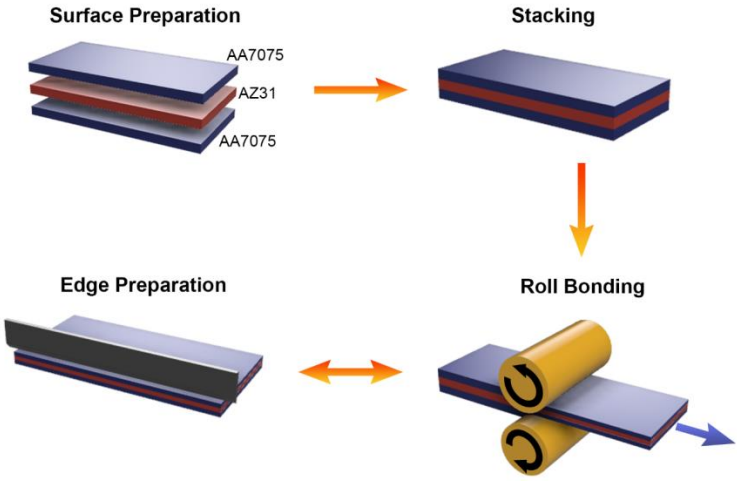


*Fig.1. Illustration of ARB process for fabricating the Al-alloy/Mg-alloy/Al-alloy composite.*

*2.6 Tensile Properties*

The tensile test was conducted to evaluate the tensile strength and ductility of the ARB composite material. In accordance with ASTM E8 specifications, tensile test specimens with a gauge length of 50 mm and a width of 12.5 mm in the rolling direction were constructed. The universal tensile testing machine (Make: Tinius Olsen; Model: H25KT) was utilized to conduct tensile tests at room temperature with a constant cross-head velocity of 0.5 mm/min. The specimens' UTS and elongation were determined using the stress-strain curve.

*2.7 Fractography*

The field-emission scanning electron microscope was used to acquire fractography of the tensile test specimens (Make: Zeiss; Model: Gemini). Using fractography, the effectiveness of the binding between alloy strips and fracture mechanism was determined.

## 3. Results and Discussion

*3.1 Accumulative Roll Bonding*

Initially, alloy strips were rolled from AA7075 and AZ31 alloy plates. The alloy strips were piled such that 3.40 mm-thick AZ31 alloy strips were sandwiched between AA7075 alloy strips. The sandwich structure was hot-rolled in numerous passes (four passes) at 400°C to make the ARB composite, with each successive pass reducing the thickness by at least 50%. The formability of materials is enhanced by performing ARB at increased temperatures [23]. The manufactured ARB composite had a thickness that was 93.5% less than that of the initially stacked metal strips.

*3.2 Microstructure*

The optical microscope image of the ARB composite specimen along its transverse slice is depicted in Figure 2. The microstructure reveals the layers of the constituent alloy strips, with AA7075 alloy strip at the top and bottom and AZ31 alloy strip in the middle. The composite's top layer was 0.08891 mm in thickness, while the middle layer measured 0.08114 mm and the bottom layer measured 0.04995 mm. The creation of additional high-angle grain boundaries during the rolling and ARB processes may have led to the production of fine-grained AZ31 [17, 24]. In addition, the grains were observed to be elongated in the rolling direction. As the number of ARB passes rises, so does the strain imposed on the composite, hence refining the grain structure [24-26]. The microstructures reveal the creation of a diffusion layer at the contact between AZ31 and AA7075. The diffusion layer had a thickness between 3 and 4 µm. Figure 3 depicts the diffusion layer zone at both interface zones with dashed lines. The applied strain and high temperature during the ARB process assisted in the diffusion and production of intermetallic compounds. Al and Mg-based intermetallic compounds could potentially develop near the AA7075 and AZ31 layers, respectively [23, 27]. Al12Mg17 and Al3Mg2 could have generated near the Mg alloy layer and Al alloy layer, respectively, according to earlier studies [19]. The production of Al-Mg intermetallic compounds at the interface as a result of atomic diffusion may indicate that the connection between the alloy layers has been strengthened [23].

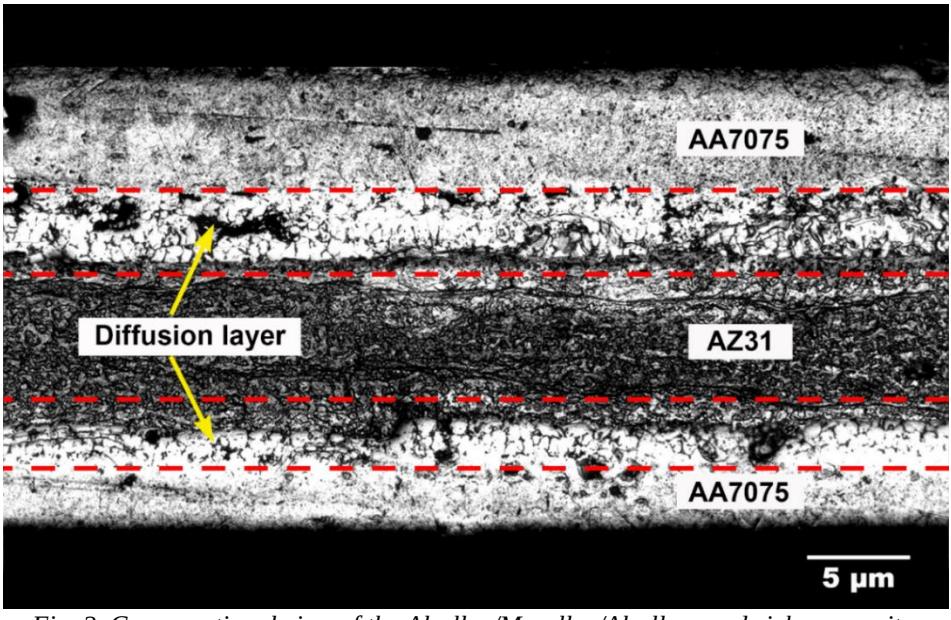


*Fig. 2. Cross-sectional view of the Al-alloy/Mg-alloy/Al-alloy sandwich composite.*

*3.3 Elemental composition*

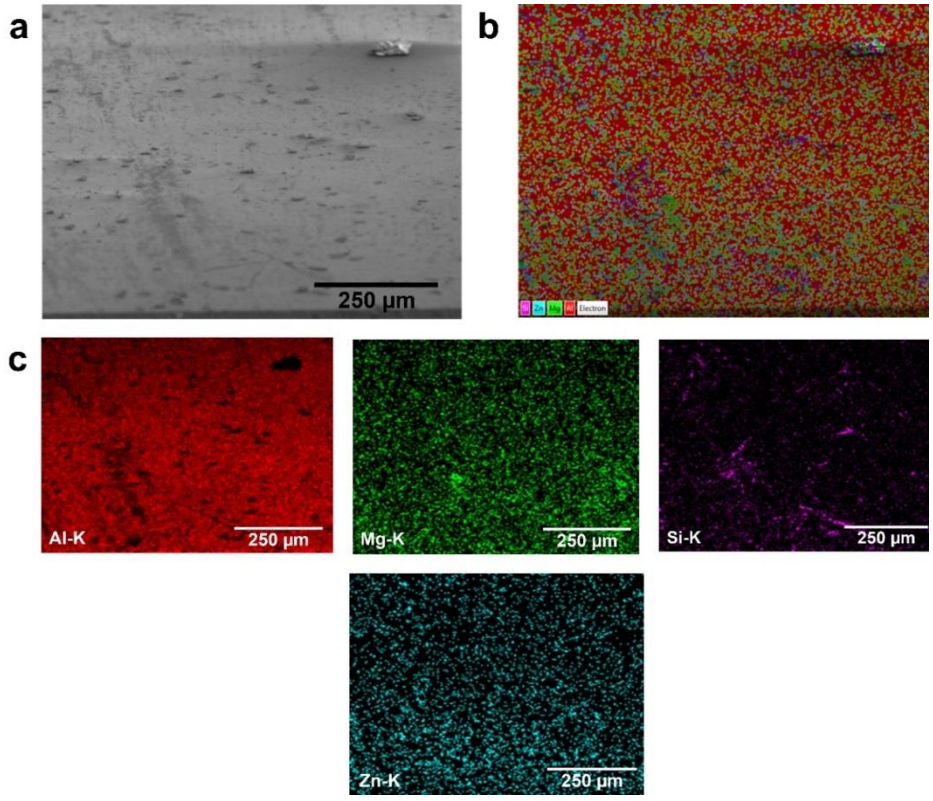


*Fig. 3. Elemental composition of ARB Composite Specimen.*

Figure 3 (a) depicts the diffusion layer of the ARB composite specimen, while Figure 3 (b) depicts the matching map of consolidated elemental composition (b). It was observed that the constituent elements were distributed homogeneously. Individual elemental maps also demonstrated the dispersion of elements between the Al alloy and the Mg alloy. The black dots and patches were intermetallic phases that had been fractured. As indicated in Figure 4, the line EDS analysis reveals the distribution of elements across the diffusion zone in the ARB composite material (a-e). Aluminium and Magnesium are the most abundant components, with trace amounts of the alloyed elements of AA7075 and AZ31 (Al, Zn, and Si) also present. In the diffusion zone, the line EDS also demonstrated the homogenous dispersion and mutual diffusion of allying components.

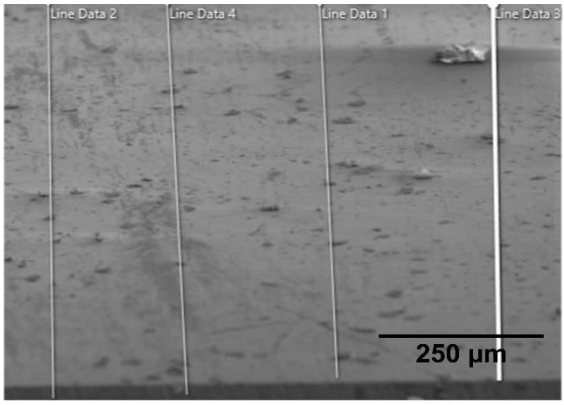
Line Data 2
Line Data 4
Line Data 1
Line Data 3
250 µm

**a**

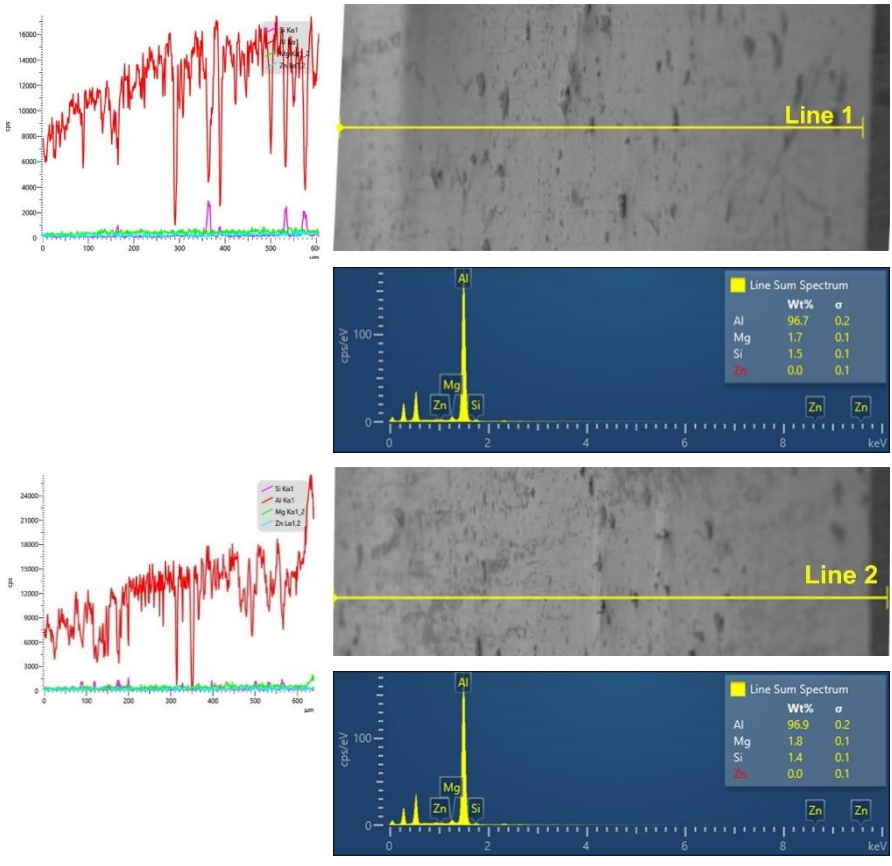
Line 1
Line Sum Spectrum
Wt% σ
Al 96.7 0.2
Mg 1.7 0.1
Si 1.5 0.1
Zn 0.0 0.1
Line 2
Line Sum Spectrum
Wt% σ
Al 96.9 0.2
Mg 1.8 0.1
Si 1.4 0.1
Zn 0.0 0.1

**b**

**c**

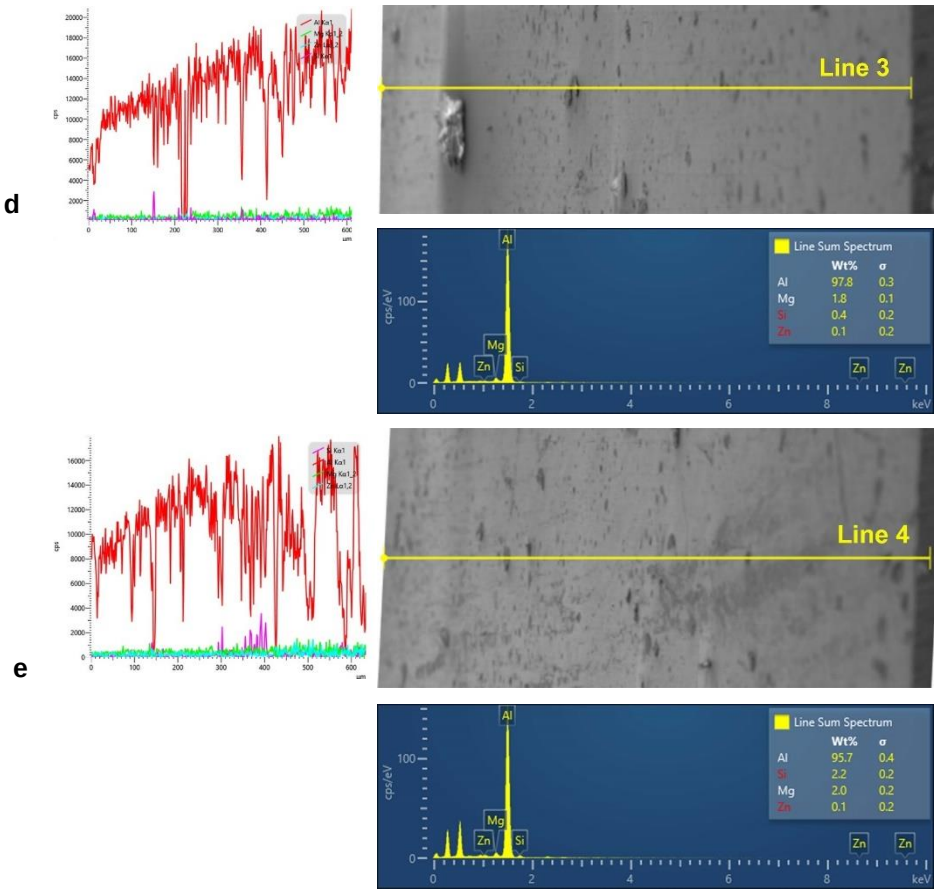


Fig. 4. Line elemental map of the ARB Composite specimen.

*3.4 Tensile Strength and Ductility*

Figure 5 depicts the usual engineering stress-strain curve of the sandwich composite. The ARB composite sample had a mean UTS of 94.7 MPa. It was anticipated that the multilayer composite formed by the ARB approach would have more strength than the separate alloys [18]. Nonetheless, the durability of the AZ31 layer diminished the composite's strength. The lengthening of the specimen was estimated to be 0.494%. The poor ductility of the composite [23, 27] could be attributed to the brittleness of AZ31 alloy and the production of intermetallic compounds at the diffusion layer.

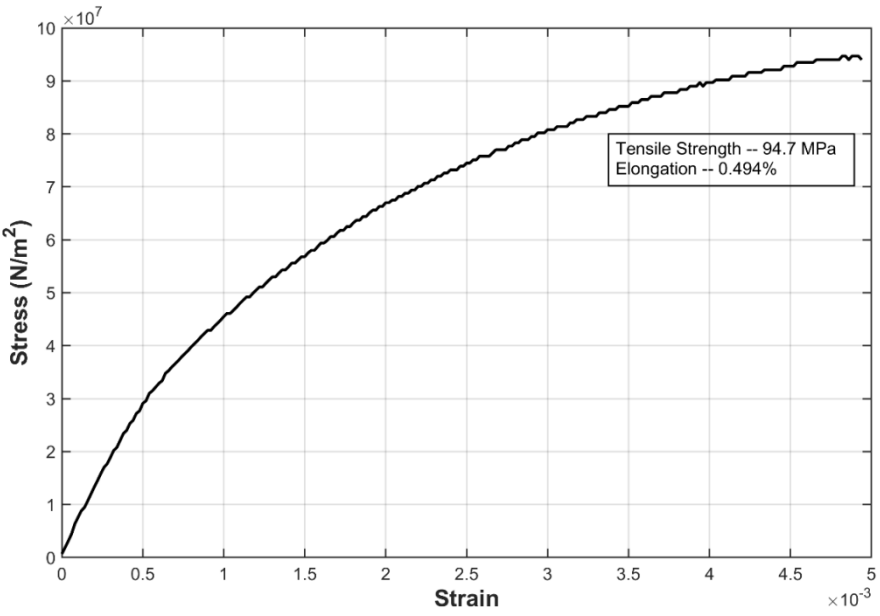


*Fig. 5. Typical stress-strain curve of the Al-alloy/Mg-alloy/Al-alloy composite.*

*3.5 Fractography*

Figure 6 depicts the fractograms of the accumulative roll-bonded specimen following tensile testing. The shattered morphology of the tensile test specimens is depicted in Figure 6 (a). The lack of undulations and peel-off layers indicated that the specimen did not delaminate during the tensile test. Figure 6 (b) and Figure 6 (c) depict an enlarged picture of the surface, which supports the absence of delamination between layers. Consequently, it is clear that AA7075 and AZ31 alloy strips have entirely bonded [28]. However, the specimen's fracture mechanism was distinct. The fractography indicates that the fractured specimen lacks distinctive dimples or plastic deformation. In addition, no cleavage steps or quasi cleavage dimples were observed on the sample. With their murky surface, Figures 6 (d) and (e) support the absence of any recognizable deformation or fracture process on the specimen. Therefore, the specimen's fracture mechanism is regarded to be complex. It is possible that both brittle and ductile modes manifested in the specimen, resulting to fracture.

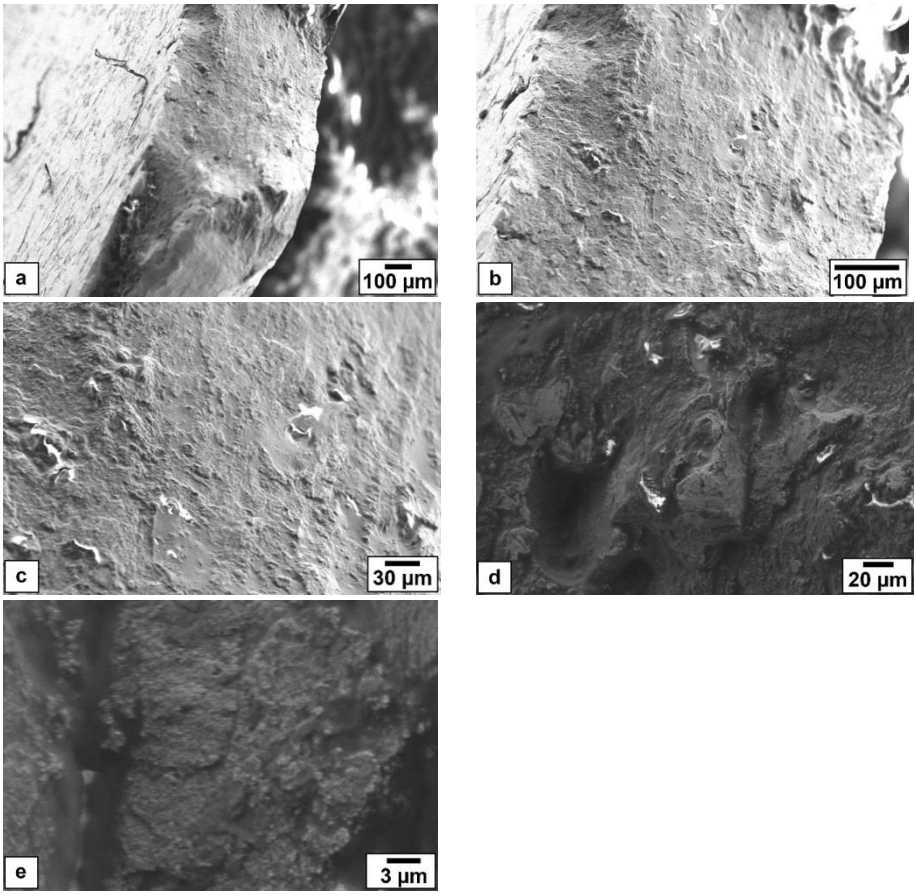


*Fig. 6. Fractography images of Al-alloy/Mg-alloy/Al-alloy sandwich composite.*

## Conclusion

The fundamental purpose of this research was to create a sandwich composite composed of three layers of Al/Mg/Al. The following conclusions were drawn from an investigation:

1. The optical micrographs depict distinct layers of alloy strip layers. A fine-grained AZ31 layer was produced, with grains elongated in the rolling direction.
2. The composite's ultimate tensile strength was determined to be 94.7 MPa following the ARB procedure.
3. The composite's 0.494% elongation was attributable to the brittle nature of the Mg alloy and the intermetallics at the interface.
4. Fractography demonstrates the occurrence of a composite failure mechanism with brittle and ductile features.

## Data Availability

The datasets generated during and/or analyzed during the current study are available from the corresponding author on reasonable request.

## Acknowledgment

The authors are grateful to Amrita Vishwa Vidyapeetham, India for their financial support to establish the High Rolling Mill Facility at Materials Processing Laboratory, Department of Mechanical Engineering, Amrita School of Engineering, Amrita Vishwa Vidyapeetham (Coimbatore Campus), India.

## References

[1] F. C. Campbell, Lightweight Materials—Understanding the Basics, https://www.asminternational.org/documents/10192/1849770/05355G_Sample.pdf, Accessed 28 May 2021.
[2] M. Govindaraju, U. Chakkingal, P. R. Kalvala, R. Vaira Vignesh, K. Balasubramanian: J Mater Eng Perform, 29 (2020) 3172-3182.
[3] R. Vaira Vignesh, R. Padmanaban, and M. Govindaraju: Bull Mater Sci, 43 (2020) 1-12.
[4] R. Vaira Vignesh, R. Padmanaban, and M. Govindaraju: Silicon, 12 (2020) 1085-1102.
[5] E. E. R. Energy, Lightweight Materials for Cars and Trucks, https://www.energy.gov/eere/vehicles/lightweight-materials-cars-and-trucks, Accessed 28 May 2021
[6] N. Rahulan, S. Gopalan, and S. Kumaran: Mater Today: Proc, 5 (2018) 17935-17943.
[7] V. Pamula, K. P. Kalyan, R. V. Vignesh, and M. Govindaraju: Mater Today: Proc, 45 (2021) 7816-7821.
[8] G. V. Kumar, C. Rao, and N. Selvaraj: Composites, Part B 43 (2012) 1185-1191.
[9] A. Graf: Materials, Design and Manufacturing for Lightweight Vehicles, Elsevier, 2021, 97-123.
[10] K. Sivanur, K. Umananda, and D. Pai, in AIP Conference Proceedings Eds. M Satyanarayana Gupta, TVK Gupta and N Kishore Nath, AIP Publishing LLC 2021 p. 020032.
[11] V. V. Ramalingam, P. Ramasamy, M. D. Kovukkal, and G. Myilsamy: Met Mater Int, 26 (2020) 409-430.
[12] D. S. Kumar, C. T. Sasanka, K. Ravindra, and K. Suman: Am J Mater Sci Technol, 4 (2015) 12-30.
[13] D. Kumar, R. K. Phanden, and L. Thakur: Mater Today: Proc 38 (2021) 359-364.
[14] G. Ghongade, K. P. Kalyan, R. V. Vignesh, and M. Govindaraju: Mater Today: Proc, 46 (2021) 4520-4526.
[15] Y. Saito, H. Utsunomiya, N. Tsuji, and T. Sakai: Acta Mater, 47 (1999) 579-583.
[16] H. Pirgazi, A. Akbarzadeh, R. Petrov, and L. Kestens: Mater Sci Eng A, 497 (2008) 132-138, 2008.
[17] D. Rahmatabadi, M. Tayyebi, R. Hashemi, and G. Faraji: Int J Miner Metall Mater, 25 (2018) 564-572.
[18] M. D. Gholami, D. Rahmatabadi, T. Shojaee, R. Hashemi, and B. Mohammadi: Mater Res Express, 8 (2021) 1-12.

[19] H. Jafarian, M. Mahdavian, S. Shams, and A. Eivani: Mater Sci Eng A, 805 (2021) 140556.
[20] D. Rahmatabadi, M. Pahlavani, M. D. Gholami, J. Marzbanrad, and R. Hashemi: J Mater Res Technol, 9 (2020) 7880-7886.
[21] Yang Wang, Yang Liao, Ruizhi Wua, Nodir Turakhodjaev, Hongtao Chen, Jinghuai Zhang, Milin Zhanga, Sharofuddin Mardonakulov: Mater Sci Eng A, 787 (2020) 139494.
[22] G. F. V. Voort: ASM Handbook Volume 9: Metallography and Microstructures, ASM International, 2004, 1058-1060.
[23] M. Abbasi and S. A. Sajjadi: J Mater Eng Perfe, 27 (2018) 3508-3520.
[24] N. Hansen, X. Huang, R. Ueji, N. Tsuji: Mater Sci Eng A, 387 (2004) 191-194.
[25] D. Rahmatabadi, R. Hashemi, B. Mohammadi, T. Shojaee: Mater Sci Eng A, 708 (2017) 301-310.
[26] D. Rahmatabadi, A. Shahmirzaloo, R. Hashemi, and M. Farahani: Mater Res Express, 6 (2019) 086542.
[27] K. Wu, H. Chang, E. Maawad, W. Gan, H. Brokmeier, and M. Zheng: Mater Sci Eng A, 527 (2010) 3073-3078.
[28] D. Rahmatabadi and R. Hashemi: Int J Mat Res, 108 (2017) 1036-1044.